

# Strain Hardening of Actin Filament Networks

REGULATION BY THE DYNAMIC CROSS-LINKING PROTEIN  $\alpha$ -ACTININ\*Received for publication, March 20, 2000, and in revised form, August 22, 2000  
Published, JBC Papers in Press, August 22, 2000, DOI 10.1074/jbc.M002377200Jingyuan Xu<sup>‡§¶</sup>, Yiider Tseng<sup>‡¶</sup>, and Denis Wirtz<sup>‡¶</sup>

From the <sup>‡</sup>Department of Chemical Engineering and Interdepartmental Program in Molecular Biophysics, The Johns Hopkins University, Baltimore, Maryland 21218 and <sup>§</sup>Biomaterials Processing Research, National Center for Agricultural Utilization Research, United States Department of Agriculture, Peoria, Illinois 61604

**Mechanical stresses applied to the plasma membrane of an adherent cell induces strain hardening of the cytoskeleton, i.e. the elasticity of the cytoskeleton increases with its deformation. Strain hardening is thought to mediate the transduction of mechanical signals across the plasma membrane through the cytoskeleton. Here, we describe the strain dependence of a model system consisting of actin filaments (F-actin), a major component of the cytoskeleton, and the F-actin cross-linking protein  $\alpha$ -actinin, which localizes along contractile stress fibers and at focal adhesions. We show that the amplitude and rate of shear deformations regulate the resilience of F-actin networks. At low temperatures, for which the lifetime of binding of  $\alpha$ -actinin to F-actin is long, F-actin/ $\alpha$ -actinin networks exhibit strong strain hardening at short time scales and soften at long time scales. For F-actin networks in the absence of  $\alpha$ -actinin or for F-actin/ $\alpha$ -actinin networks at high temperatures, strain hardening appears only at very short time scales. We propose a model of strain hardening for F-actin networks, based on both the intrinsic rigidity of F-actin and dynamic topological constraints formed by the cross-linkers located at filaments entanglements. This model offers an explanation for the origin of strain hardening observed when shear stresses are applied against the cellular membrane.**

Cells are continuously subject to mechanical stresses generated by internal and external forces (1). To spread, migrate, maintain tissue shape (4), or to resist the shear forces of blood flow (5), these forces are applied against adhesive contacts formed by the cell with the extracellular matrix (2, 3) or with neighboring cells. Filamentous actin (F-actin),<sup>1</sup> which is one of the major components of cortical cytoplasm and focal adhesions, is believed to play a key role in the mechanical response of cells (6). The assembly/disassembly or the severing/annealing/capping of actin filaments, which are regulated by actin-binding proteins (7, 8), constitute mechanisms of fast “sol-gel” transitions of cytoplasm to potentiate the cell’s response to mechanical stresses. However, as shown below, dynamic F-

actin cross-linkers such as the protein  $\alpha$ -actinin may provide the cell with an alternative and/or complementary mode of sorting out mechanical perturbations, based on their rate and magnitude, and instantaneously either resisting stresses or helping locally liquefy the F-actin network.

The local response of a cell subject to mechanical stresses has been studied using biophysical techniques, including magnetic twisting cytometry (9) and magnetic tweezers (10). Wang *et al.* (9) used beads coated with multivalent fibronectin (FN) or RGD peptide to locally form an actin-rich focal contact (11, 12). Twisting the beads induced strain hardening of the cytoskeleton, i.e. the cytoskeleton’s elasticity increased when it was deformed (9). The origin of this strain-hardening behavior was attributed to the tensegrity of the cell (9, 13). The inter-connected, geodesic-like organization of the cytoskeleton would induce enhanced mechanical resilience when the cell is deformed, which, in turn, is thought to promote the transduction of mechanical signals across the plasma membrane through the cytoskeleton, to the nucleus (9, 13). However, Bausch *et al.* (10), who applied applying shear forces using FN-coated magnetic beads, did not observe any strain hardening. They found instead that shear forces applied to the plasma membrane induced softening of the cytoskeleton, i.e. applied deformations decreased the cytoskeleton’s local modulus.

We used reconstituted F-actin networks to help resolve these apparently contradictory results and to model the mechanical response of the actin network under deformation. Rheological measurements have shown that actin filaments form relatively weak gels even at high (physiological) concentrations (shear modulus  $G \approx 50$  dynes/cm<sup>2</sup> for a 5–10 mg/ml F-actin solution) (14). Hence, auxiliary F-actin-binding proteins are required to cross-link and/or bundle actin filaments into stiff arrays to help maintain cell morphology against mechanical stresses. However, little is known about the effect of shear deformations on the behavior of F-actin networks *in vitro*. The effect of applied stresses on the viscoelastic response of reconstituted F-actin networks has been studied in the presence of the F-actin bundling protein, ABP-280 (15), and calponin/ $\alpha$ -actinin (16). In both cases,  $G'$  and  $G''$ , the storage and loss moduli, were computed as a function of the strain amplitude  $\gamma_0$  by subjecting the network to sinusoidal deformations,  $\gamma(t) = \gamma_0 \sin \omega t$ , of a single frequency  $\omega$ . For small amplitude oscillatory deformations,  $G'$  and  $G''$  increased for increasing  $\gamma_0$ , i.e. the F-actin network exhibited strain hardening and the network’s resilience was enhanced when deformed. Instead, for large amplitudes,  $G'$  and  $G''$  decreased for increasing  $\gamma_0$ , i.e. the F-actin network softened, which was attributed to the breakage of the filaments by shear (15, 16). Using the same assay, it was also found that F-actin alone exhibited strong strain hardening (17, 18) (see more under “Discussion”).

\* The costs of publication of this article were defrayed in part by the payment of page charges. This article must therefore be hereby marked “advertisement” in accordance with 18 U.S.C. Section 1734 solely to indicate this fact.

<sup>¶</sup> Both authors contributed equally to this work.

<sup>§</sup> Supported by National Science Foundation Grant CTS9812624 and by NASA Grant NAG81377. To whom correspondence should be addressed: Tel.: 410-516-7006; Fax: 410-516-5510; E-mail: wirtz@jhu.edu.

<sup>1</sup> The abbreviations used are: F-actin, filamentous actin; G-actin, monomeric actin in buffer G; FN, fibronectin.

To assess the effect of strain on the mechanical response of cross-linked and uncross-linked F-actin networks, we employed step deformations, which provided insight into the dynamics of actin filaments under shear. We investigated the mechanical response of a model system consisting of actin filaments and the F-actin cross-linking protein  $\alpha$ -actinin, a protein that transiently binds F-actin and that localizes along contractile stress fibers and at focal adhesions (19, 20).  $\alpha$ -Actinin molecules consist of two identical polypeptides of 103 kDa with a 30-kDa N-terminal actin-binding domain, a tail with triple helical repeats, and two C-terminal EF-hands (19). The rod-shaped tails associate to form an anti-parallel dimer with an actin filament binding site on each end. Sato *et al.* (21) and Wachsstock *et al.* (22) have already showed that both *Acanthamoeba* and chicken  $\alpha$ -actinin enhance the elasticity of F-actin networks in the linear regime, for which moduli are strain-independent. Here, we extended these studies to the non-linear regime, tested *in vivo* by Wang *et al.* (9) and Bausch *et al.* (10), for which moduli become functions of the imposed deformation.

#### MATERIALS AND METHODS

**Protein Purification**—Unless specified, all reagents were purchased from Sigma (St. Louis, MO). Actin was prepared from rabbit skeletal muscle (23) using Sephacryl S-300 for gel filtration (24). Purified actin was stored as  $\text{Ca}^{2+}$ -actin in continuous dialysis at 4 °C against buffer G (0.2 mM ATP, 0.5 mM dithiothreitol, 0.2 mM  $\text{CaCl}_2$ , 1 mM sodium azide, and 2 mM Tris-HCl, pH 8.0).  $\text{Mg}^{2+}$ -actin filaments were generated by adding 0.1 volume of 10-X KMEI (500 mM KCl, 10 mM  $\text{MgCl}_2$ , 10 mM EGTA, 100 mM imidazole, pH 7.0) polymerizing salt buffer solution to 0.9 volume of G-actin in buffer G. Actin filament networks were not supplemented with the stabilizing agent phalloidin, which can substantially change the bending rigidity of the filaments (25).  $\alpha$ -Actinin was purified from chicken smooth muscle (26) and stored by dialysis against buffer G, which was changed daily with fresh buffer. Proteins were used within 5 days of purification (27).

**Rheological Methods**—The strain-dependent properties of cross-linked and uncross-linked F-actin networks at steady state were measured with a cone-and-plate, strain-controlled, fluid rheometer (ARES 100, Rheometrics Inc., Piscataway, NJ), described previously (14, 28). Monomeric actin in buffer G (G-actin) was mixed with one-tenth volume of 10-X KMEI to a final concentration of 24  $\mu\text{M}$  ( $\approx 1$  mg/ml) and immediately placed between the temperature-controlled cone and plate of the rheometer. The extent of gelation of actin in the presence or absence of  $\alpha$ -actinin was monitored by measuring the storage and loss moduli,  $G'$  and  $G''$ , every 30 s for 6 h. After steady state was reached (*i.e.* after  $G'$  and  $G''$  reached a steady-state plateau), we conducted stress-relaxation experiments where the time-dependent stress,  $\sigma(t)$  (force per unit area), was measured after a step strain (*i.e.* a suddenly applied shear deformation) of controlled amplitude  $\gamma_0$  was applied and maintained for 1000 s (illustrated below in Fig. 2*a*). The time after application of the step deformation represents a time scale that describes the motion of the filaments in the network (see “Discussion”) and is equivalent to the inverse of the frequency in an oscillatory assay,  $t = 2\pi/\omega$ . The relaxation modulus  $G(t, \gamma_0)$  reported here is the ratio  $\sigma(t)/\gamma_0$ . Because large deformations may break actin filaments, a new stress-relaxation experiment was not conducted until the overall viscoelastic modulus,  $|G^*| = \sqrt{G'^2 + G''^2}$  (evaluated at  $2\pi$  rad/s and  $\gamma_0 = 1\%$ ), measured during recovery after a stress-relaxation measurement, was less than 10% away from the modulus  $G$  (evaluated at 1 s) measured during the 1% amplitude step-relaxation experiment. From these stress-relaxation measurements, we extracted the modulus  $G(t, \gamma_0)$  as a function of strain amplitude  $\gamma_0$  (see Figs. 1*d*, 2*b*, 4*a*, and 4*b*), time scale (see Figs. 2*a* and 3), and temperature (see Figs. 2 and 3). The behavior of F-actin solutions during oscillatory deformations was probed (with a different aliquot) by applying a sinusoidal deformation,  $\gamma(t) = \gamma_0 \sin \omega t$ , of fixed frequency  $\omega = 1$  rad/s and increasing strain amplitude  $\gamma_0$ , and measuring the induced time-dependent stress,  $\sigma(t)$  (illustrated in Fig. 1, *a* and *e*). To compare strain-dependent moduli obtained with the just-described step deformation assay and moduli obtained with the more traditional “strain-sweep” assay (15, 16), different aliquots of F-actin networks were also subject to a couple of sine deformations of a frequency of 1 rad/s and increasing amplitudes (see Fig. 1*d*). To test the mechanical properties of F-actin in the presence  $\alpha$ -actinin, we premixed  $\alpha$ -actinin with G-actin, added 10-X KMEI, and immediately inserted the mixture into the rheometer. A molar ratio [ $\alpha$ -actinin]:[actin] of 1:50 was chosen

to test the mechanical properties under conditions where actin filaments did not exhibit extensive bundling (22, 29, 30).

#### RESULTS

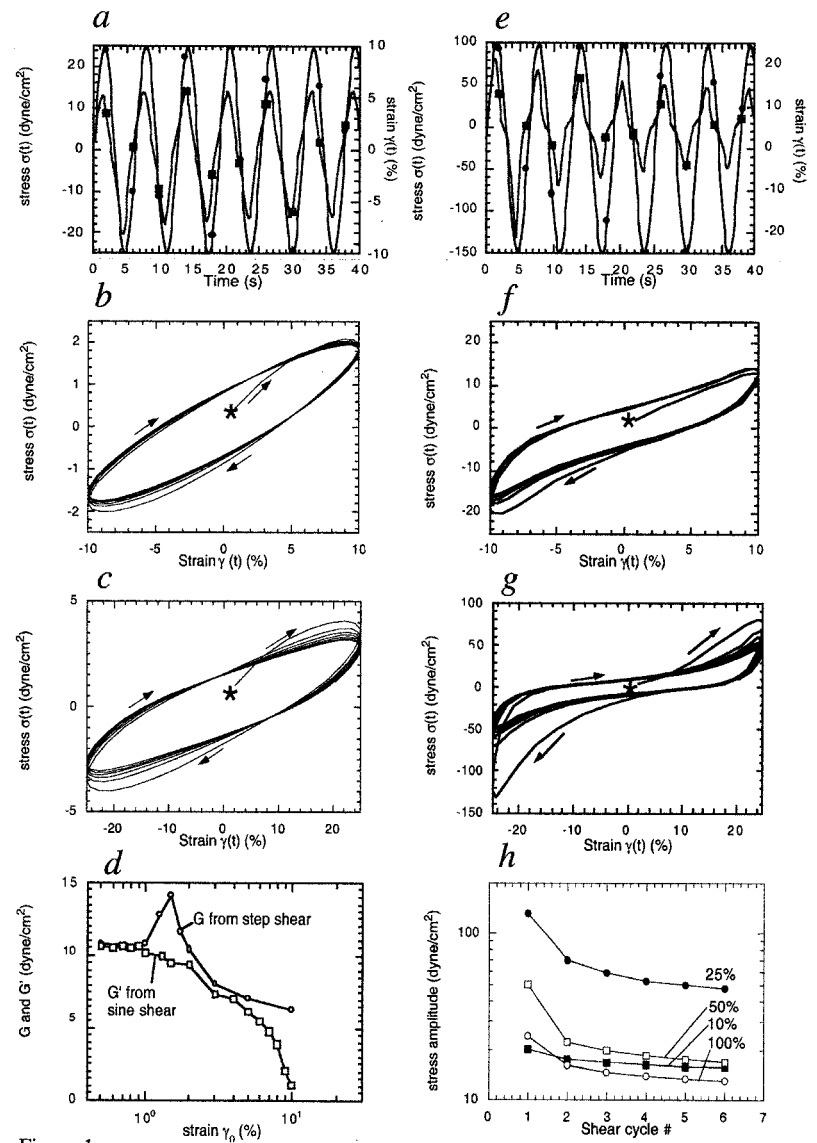
**Sinusoidal versus Step Deformation of F-actin**—The effect of deformation amplitude on the mechanical properties of F-actin networks is often assessed by subjecting them to oscillatory deformations,  $\gamma(t) = \gamma_0 \sin \omega t$ , of fixed frequency  $\omega$  and increasing amplitudes  $\gamma_0$  (15–18). Viscoelastic moduli are calculated from either the maximum amplitudes or the time-averaged amplitudes of the in-phase and out-of-phase components of the (presumably) sinusoidal stress over a few (typically two to three) cycles of shear. For small  $\gamma_0$ , the moduli are independent of  $\gamma_0$ , which defines the linear regime. However, for large  $\gamma_0$ , the network may soften during the assay itself. To show this effect, we monitored the evolution of the viscoelastic response of F-actin during an oscillatory deformation and measured the corresponding time-dependent shear stress,  $\sigma(t)$  (Fig. 1*a*). We observed that, although the input deformation was perfectly sinusoidal, the output stress was not; the amplitudes of stress oscillations became smaller over time (Fig. 1*a*).

To better analyze the behavior of F-actin subject to oscillatory deformations, we replotted  $\sigma(t)$  as a function of  $\gamma(t)$  to generate Lissajoux figures (see Ref. 28 for more details), where time runs along the curve clockwise (Fig. 1, *b* and *c*). At short times during the first cycle of shear, the stress increased linearly with the applied deformation, *i.e.* the corresponding modulus,  $G(t) = \sigma(t)/\gamma(t)$ , was independent of shear (Fig. 1*b*). During the same first cycle of shear, however, the stress started increasing more slowly than the applied strain, *i.e.* F-actin “yielded.” For subsequent cycles of oscillatory shear, the Lissajoux figure slightly rotated clockwise, because the F-actin solution softened over time (Fig. 1*b*), which was also reflected by the decrease of the amplitudes reached during the oscillations of  $\sigma(t)$  (Fig. 1*a*). This trend was enhanced for oscillatory deformations of larger amplitudes (Fig. 1*c*).

F-actin networks cross-linked with  $\alpha$ -actinin were also sensitive to oscillatory shear deformations: a sinusoidal deformation did not produce a sinusoidal stress either (Fig. 1*e*). Here, during the first cycle of shear, the effective modulus  $G(t)$  was initially constant, because the stress increased linearly with the applied deformation but increased steeply at later times (Fig. 1*f*); therefore, F-actin became strain-hardened. Although the overall axis of the Lissajoux figure rotated clockwise, which indicated progressive softening, an  $\alpha$ -actinin cross-linked F-actin network continued to exhibit strain hardening at the end of each cycle of shear (Fig. 1, *f* and *g*). Hence, with or without  $\alpha$ -actinin, a couple of shear oscillations is sufficient to change the stiffness of F-actin.

Due to the non-periodicity of  $\sigma(t)$ , storage and loss moduli,  $G'$  and  $G''$ , are ill-defined, because the probing shear itself changed the amplitudes of the stress during the assay (Fig. 1, *a*, *e*, and *h*). For large amplitudes, non-periodicity became pronounced (Fig. 1, *c* and *g*). Therefore, repeated oscillatory deformations are typically inappropriate to analyze the strain dependence of  $G'$  and  $G''$  and quantitatively assess the effect of strain amplitude on the mechanical behavior of F-actin solutions. In addition, it would be extremely time-consuming to sequentially subject F-actin to deformations of different frequencies and strain amplitudes. For a fixed strain amplitude, a stress relaxation experiment probed over a 0.01- to 100-s time scale range lasts 100 s; instead, a frequency-based experiment with frequencies between 0.01 and 100  $\text{s}^{-1}$  (equivalent to the 0.01- to 100-s time scale range) lasts  $\approx 1$  h, conservatively probing three frequencies per decade with two oscillations per frequency. Hence, if for instance 10 strain amplitudes were to be probed, stress-relaxation experiments would last just 1000 s

**FIG. 1. Mechanical behavior of F-actin networks subject to oscillatory deformations.** The conditions are  $24 \mu\text{M}$  actin with or without  $0.48 \mu\text{M}$  chicken smooth muscle  $\alpha$ -actinin. Networks were subject to sinusoidal deformations,  $\gamma = \gamma_0 \sin \omega t$ , of fixed frequency  $\omega = 1 \text{ rad/s}$  and increasing deformation amplitude  $\gamma_0$ . *a*, time-dependent strain,  $\gamma(t)$  (●), and induced stress,  $\sigma(t)$  (■), for F-actin alone;  $\gamma_0 = 10\%$ . *b*, Lissajoux figure:  $\sigma(t)$  versus  $\gamma(t)$ . Same conditions as in *a*. *c*, Lissajoux figure for  $\gamma_0 = 25\%$ . Same conditions as in *a*. *d*, comparing moduli obtained from step strain deformations (○) and from frequency-based assay (□) (see text for details). *e*,  $\gamma(t)$  (●) and  $\sigma(t)$  (■) for F-actin +  $\alpha$ -actinin;  $T = 25^\circ\text{C}$ ;  $\gamma_0 = 25\%$ . *f*, Lissajoux figure for  $\gamma_0 = 10\%$ . *g*, Lissajoux figure for  $\gamma_0 = 25\%$ . Same conditions as in *e*. Arrows in *b*, *c*, *f*, and *g* indicate the sense of evolution; the star indicates time 0. *h*, amplitudes of the stress versus cycle number for F-actin +  $\alpha$ -actinin subject to various strain amplitudes. Symbols are  $\gamma_0 = 10\%$  (■),  $25\%$  (●),  $50\%$  (□), and  $100\%$  (○).



$\approx 17$  min, while frequency-based experiments would last  $\approx 10$  h. We therefore used a step deformation assay to probe both the strain dependence and the time scale dependence of the viscoelastic moduli of F-actin networks.

**F-actin Network Exhibited Strain hardening**—F-actin rheology in the linear regime, for which deformations are small enough so that moduli remain independent of the applied strain, has been extensively studied (see Ref. 27 and references therein). Here, to focus on the dependence of F-actin mechanical behavior on deformation, we employed step deformations (see “Materials and Methods”) and monitored the relaxation of the induced stress (Fig. 2*a*). Step deformations have the advantage, over oscillatory deformations, to subject F-actin networks to smaller overall deformations, to measure stresses in real time, and to probe the time scale dependence of the mechanical response (31). Moreover, oscillatory deformations of increasing deformation amplitudes exhibit increasing rates of deformation, because the rate is proportional to  $\gamma_0$ ,  $d\gamma/dt = \gamma_0 \omega \cos(t)$ . The modulus of an F-actin network displayed the same overall relaxation profile at all tested deformations: the modulus of an F-actin network first relaxed rapidly, up to time scales of about 10 s, then reached a quasi-plateau, which extended from about 10 to 1000 s (Fig. 2*a*) and finally underwent a terminal relaxation for  $t > 1000$  s (not shown here). Strain-dependent moduli at a given time scale were directly obtained from relaxation

moduli (Fig. 2*b*) by extracting the corresponding value of  $G$  from Fig. 2*a* at different strain amplitudes. The modulus of F-actin remained independent of strain amplitude for strains up to  $\gamma_0 \approx 1\%$ , which defined the extent of the linear regime (Fig. 2*b*). However, the modulus increased 8–31% (depending on the time scale) with strain amplitudes between 1 and 1.5% and decayed slowly for strain higher than  $\gamma_c \approx 1.5\%$  (Fig. 2*b*). Note that values of the yield strain varied  $\approx 50\%$  from experiment to experiment (data not shown). We suggest that the bending rigidity of F-actin is responsible for this strain hardening phenomenon (see “Discussion”). The characteristic “yield” strain  $\gamma_c$  is defined here as the strain at which the modulus started decreasing (onset of shear softening). When F-actin was tested using a frequency-based assay, we observed no strain hardening, because oscillatory deformations liquefied the network during the assay itself (Fig. 1*d*). In summary, an F-actin network behaved like a “linear” material for small strain amplitudes (*i.e.* modulus was independent of strain), exhibited strain hardening for intermediate strains, and softened slowly for large strains.

**$\alpha$ -Actinin Enhanced the Strain-dependent Mechanical Properties of F-actin**— $\alpha$ -Actinin enhanced dramatically the strain-dependent behavior of F-actin networks. First of all, in the linear regime, the elastic modulus increased in the presence of  $\alpha$ -actinin in agreement with the results of Xu *et al.* (20) (Figs.

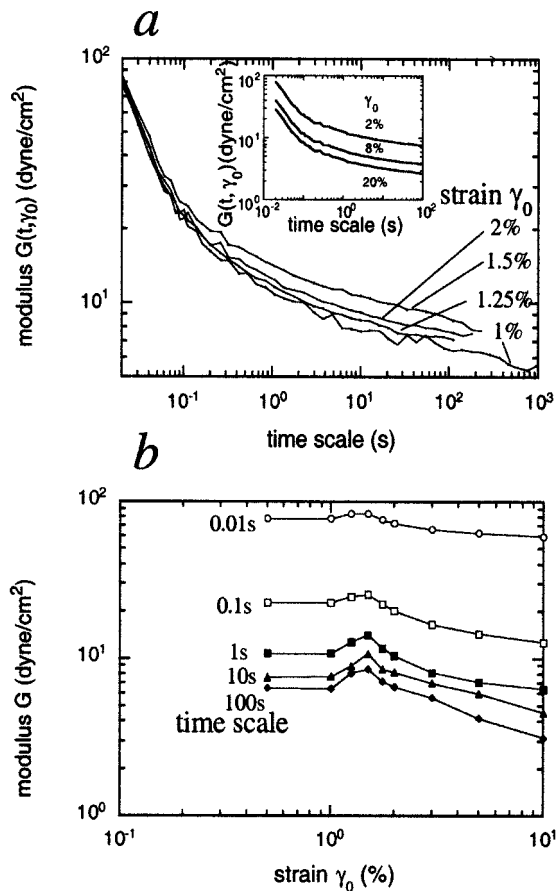


FIG. 2. **Stress relaxation in F-actin networks.** The relaxation modulus,  $G(t, \gamma_0)$ , is measured immediately following the application of step strains of amplitude  $\gamma_0$ . *a*, measured  $G(t, \gamma_0)$  as a function of time for various strain amplitudes. *Inset*,  $G(t, \gamma_0)$  for large strain amplitudes  $\gamma_0$ . *b*,  $G(t, \gamma_0)$  as a function of strain amplitude for various time scales. *b* was directly obtained from *a*. Actin concentration was  $24 \mu\text{M}$ .

2*a* and 3*a*). This enhancement of the modulus is not due to the applied strain (because it is the linear regime) but is due to the restricted motion of the filaments mediated by  $\alpha$ -actinin (see “Discussion”). More importantly for the present paper,  $\alpha$ -actinin-cross-linked F-actin networks stiffened greatly when the amplitude of the deformation was increased up to a yield strain amplitude,  $\gamma_c$ , which depended on time scale (Fig. 3, *a* and *b*). At short time scales ( $t < 1$  s), *i.e.* at high rates of shear  $\omega > 1 \text{ s}^{-1}$ , strain hardening was pronounced and  $G$  increased up to 250% compared with its value at low strains (Fig. 3, *a* and *b*). Strain hardening vanished entirely at an intermediate time scale,  $t \approx 1$  s, for which all stress-relaxation curves met (Fig. 3*a*). At long time scales ( $t > 1$  s), *i.e.* at low rates of shear,  $G$  was  $\gamma_0$ -independent up to  $\gamma_c \approx 2\%$  and decreased monotonically and precipitously thereafter (Figs. 3*b* and 4*a*). Of note, the rate at which the modulus declined beyond  $\gamma_c$  was much higher in the presence of  $\alpha$ -actinin (Fig. 4*a*) than for F-actin alone (Fig. 2*b*). Therefore,  $\alpha$ -actinin not only enhanced the strain hardening of F-actin, particularly at high rates of shear, but also allowed F-actin to withstand larger deformations.

**Temperature Regulated  $\alpha$ -Actinin-induced Strain hardening**—Here, we show that the temperature-dependent binding lifetime of  $\alpha$ -actinin to F-actin regulates strain hardening. In the absence of  $\alpha$ -actinin, the mechanical properties of F-actin solutions vary by less than 10% with temperature over the range of 8–40 °C (20). To probe the effect of temperature, and therefore the influence of  $\alpha$ -actinin’s lifetime of binding, on the strain-dependent behavior of  $\alpha$ -actinin cross-linked F-actin so-

lutions, we conducted stress-relaxation experiments at 15 and 25 °C. The extent of the plateau modulus, loosely defined as the time span over which  $G$  was approximately constant (32), was slightly reduced in the presence of  $\alpha$ -actinin at 25 °C compared with 15 °C (Fig. 3, *a* and *c*). Moreover, the plateau modulus was decreased from 66 to  $\approx 30$  dynes/cm<sup>2</sup> when the temperature was increased from 15 to 25 °C (Fig. 3, *a* and *c*). For a solution of purified F-actin, the yield strain,  $\gamma_c \approx 2\%$ , remained relatively constant for time scales between 0.01 and 100 s (Fig. 4*c*). In the presence of  $\alpha$ -actinin at 15 °C,  $\gamma_c$  increased 7-fold, from 2 to 14%, for time scale 0.01–1 s, but decreased rapidly for  $t > 3$  s and down to 2% at 10 s (Fig. 4*c*). Instead, at high temperatures,  $\gamma_c$  decreased from  $\approx 11$  to 2% for time scales between 0.01 and 0.05 s and remained constant for  $t > 0.05$  s (Fig. 4*c*). Therefore, the amplitude of shear deformation at which an F-actin network yields (*i.e.* the network’s ability to withstand deformations) increased in the presence of  $\alpha$ -actinin and decreased with the solution temperature and the probed time scale.

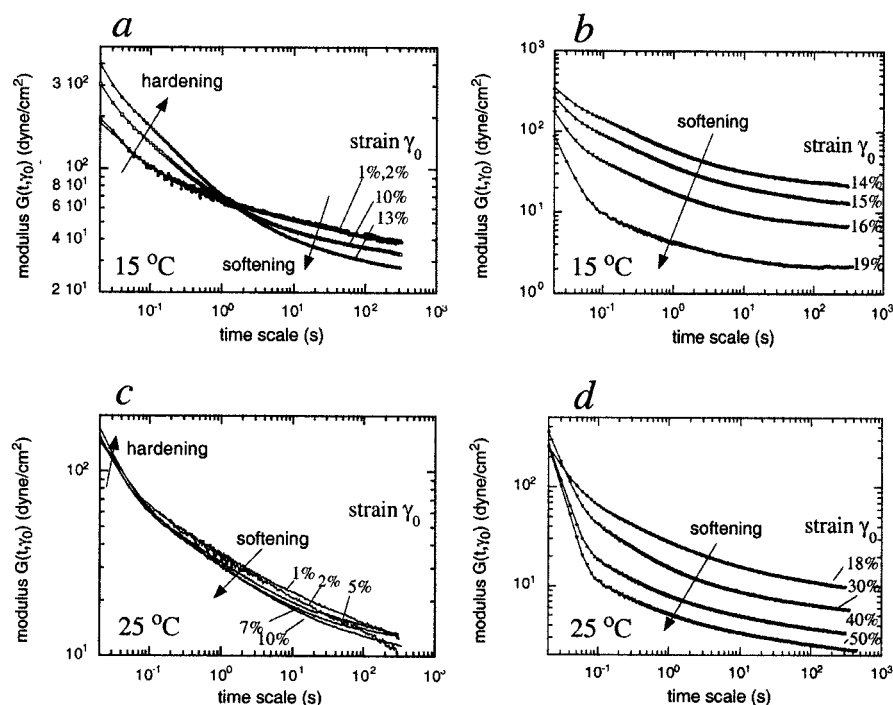
## DISCUSSION

Using rheological methods, we showed that F-actin networks strain-hardened and that the cross-linking protein  $\alpha$ -actinin could enhance this strain-dependent behavior. We showed that methods to measure the strain dependence of F-actin stiffness, which involve oscillatory deformations, could be misleading, because a sinusoidal deformation does not necessarily induce a sinusoidal stress in F-actin, particularly in the presence of an F-actin cross-linker. At low temperatures, for which the lifetime of binding of  $\alpha$ -actinin for F-actin is long, F-actin/ $\alpha$ -actinin networks stiffened for increasing shear deformations at short time scales and softened rapidly at long time scales. For cross-linked F-actin networks at high temperatures, strain hardening appeared only at very short time scales and F-actin networks softened slowly at long time scales.

**Proposed Mechanism of F-actin Strain hardening**—F-actin has previously been reported to stiffen under shear; the elastic modulus has been shown to increase from  $G' \approx 250$  to 340 dynes/cm<sup>2</sup> (evaluated at  $\omega = 1$  rad/s) for strain deformations between 1 and 10% (17). However, these results are questionable for two reasons. First, the actin used in those experiments is now known to exhibit high levels of thiol oxidation due to actin aging, which promoted G-actin dimer formation, and in turn artificially cross-linked actin filaments very effectively (18), which greatly enhanced strain hardening (as shown here in Fig. 4). Second, the assay used in the aforementioned experiments involved oscillatory deformations, which, our experiments showed, soften F-actin during the assay itself. Therefore, we turned to a step deformation assay to probe the effect of strain amplitude on the mechanical behavior of F-actin solutions.

A step deformation assay provides direct insight into the propensity of actin filaments to move within a network (33). Upon step deformation, a filament network will immediately exhibit a shear stress, which is energetically unfavorable and has to be dissipated; hence, the filaments move to relax the stress as rapidly as possible. Each actin filament imbedded in a network forms entanglements with surrounding filaments, which inhibit its motion laterally (see model in Fig. 5*a*). These entanglements form a tube-like region that confines each filament to lateral bending fluctuations at short time scales, until these lateral excursions touch the tube walls, and to longitudinal diffusion (“reptation”) at long time scales (33, 34). Therefore, the time-dependent modulus,  $G(t, \gamma_0)$ , shown in Figs. 2 and 3 simply describes bending fluctuations of the filaments at short time scales (which can be probed by particle-tracking microrheology and diffusing wave spectroscopy (14, 35, 36))

**FIG. 3. Stress relaxation in F-actin/ $\alpha$ -actinin networks: temperature dependence.** The conditions were  $24 \mu\text{M}$  F-actin +  $0.48 \mu\text{M}$   $\alpha$ -actinin at  $T = 15^\circ\text{C}$  (*a* and *b*) and  $25^\circ\text{C}$  (*c* and *d*). *a*, relaxation modulus,  $G(t, \gamma_0)$ , as a function of time for  $\gamma$  ranging from 1 to 13%. *b*,  $G(t, \gamma_0)$  for  $\gamma_0$  ranging from 14 to 19%. *c*,  $G(t, \gamma_0)$  for  $\gamma_0$  ranging from 1 to 10%. *d*,  $G(t, \gamma_0)$  for  $\gamma_0$  ranging from 18 to 50%. Arrows indicate increasing deformation amplitudes.



and the probability that the filament is still inside the initial tube at long time scales. Based on this physical insight, it was predicted that  $G(t)$  for F-actin relaxes as  $\propto t^{-3/4}$  at short time scales and reaches a plateau modulus, which depends on concentration as  $G(c) \propto c^{7/5}$  at longer time scales (34, 37, 38). These predictions were experimentally verified (14, 35, 39, 40), which strongly support the notion that, unlike the cytoskeletal filamentous proteins keratin, vimentin, and neurofilament (28, 32, 41), purely steric interactions dominate the motion of filaments and, therefore, the rheology of F-actin at small deformations.

These steric interactions and F-actin's intrinsic rigidity are likely to be also responsible for the strain hardening behavior of F-actin solutions. F-actin is a semiflexible polymer, because its persistence length,  $L_p \approx 17 \mu\text{m}$ , is of the same order of magnitude as its contour length,  $L \approx 10\text{--}15 \mu\text{m}$ , *in vitro* (42). Consider an individual actin filament imbedded in a semidilute solution (see model in Fig. 5*a*). Following a step deformation (shown in Fig. 5*b*), *i.e.* that polymer may exhibit more highly curved segments around entanglements (noted by *stars* in Fig. 5*b*), which are energetically unfavorable because of the intrinsic rigidity of F-actin. Therefore, F-actin resists further deformation, which gives rise to strain hardening. For large shear deformations, the F-actin network eventually breaks and/or flows, indicated by a drop in  $G$  versus  $\gamma_0$  past the yield strain  $\gamma_c$  (Fig. 2*b*). Instead, flexible polymers of contour length similar to F-actin (but much smaller persistence length) subject to shear can stretch coiled segments and can easily slide past one another under shear, because shear-induced bending of polymer subsections does not require much energy. For instance, solutions of flexible polymers, such as uncross-linked solutions of DNA ( $L \approx 17 \mu\text{m} \gg L_p \approx 0.05 \mu\text{m}$ ), do not exhibit strain hardening (43). Therefore, strain hardening in semidilute solutions of F-actin partly originates from the finite rigidity of actin filaments. Nevertheless, flexible polymers can also exhibit strong strain hardening, but only in the presence of cross-linkers or via non-steric interactions, which act as cross-linkers. For instance, suspensions of K5–K14 keratin filaments, which are flexible polymers ( $L \approx 2 \mu\text{m} \gg L_p \approx 0.1 \mu\text{m}$ ), stiffen under repeated shear deformations because of strong cross-linking interactions among filaments (28, 32). Once deformed,

a cross-linked flexible polymer cannot slide past entanglement points made with surrounding polymers, and therefore, resists further deformation, leading to strain hardening (see more below).

*Strain Hardening and the Binding Lifetime of  $\alpha$ -Actinin to F-actin*—At low temperatures,  $\alpha$ -actinin-mediated F-actin cross-linking greatly enhanced strain hardening: The modulus increased much more steeply with strain than for F-actin alone. At high temperatures, F-actin adopted a behavior intermediate between those of F-actin alone and F-actin +  $\alpha$ -actinin at low temperatures. Here, we attempt to relate the extent of strain hardening to the lifetime of binding of  $\alpha$ -actinin to F-actin, which decreases for increasing temperatures (20, 44). Previously, it was shown that  $k_-$ , not the overall affinity,  $K_D = k_-/k_+$ , governs the mechanical behavior of actin gels in the presence of chicken smooth muscle  $\alpha$ -actinin (20). Assuming univalent association rate constants (which should be appropriate for dilute samples) of  $k_+ = 1.4$  and  $2.7 \mu\text{M}^{-1} \text{s}^{-1}$  (corrected for the diffusion coefficient of the native protein) (29) at 15 and  $25^\circ\text{C}$ , respectively, the dissociation rate constants are  $k_- = 0.8 \pm 0.04$  and  $2.4 \pm 0.1 \text{s}^{-1}$  for smooth muscle  $\alpha$ -actinin (20). The  $\alpha$ -actinin molecules that contribute to F-actin rheology will co-localize with entanglements between actin filaments. The model in Fig. 5 predicts that at time scales shorter than  $1/k_-$ , *i.e.* shorter than  $\approx 1.3 \text{s}$  and  $0.4 \text{s}$  at 15 and  $25^\circ\text{C}$ , respectively, cross-linkers located at filament entanglements should greatly enhance F-actin resistance to shear by preventing the filaments to slide past one another (indicated by *crossed double arrows* in Fig. 5*b*). In addition, the extension of subsections of an actin filament between cross-linkers (*double-headed arrow* in Fig. 5*b*), which would be allowed by polymer sliding, also becomes greatly inhibited at short time scales. The fact that F-actin strain-hardens for time scales shorter than 1 and  $0.05 \text{s}$  at 15 and  $25^\circ\text{C}$  (Fig. 4, *a* and *b*), respectively, gives credence to this model. Differences between the times at which F-actin/ $\alpha$ -actinin strain-hardens and  $1/k_-$  may be attributed to variations in reported values of  $k_-$  for  $\alpha$ -actinin (listed in Ref. 20), to the fact that reported values are for the actin-binding domain of  $\alpha$ -actinin not for the full  $\alpha$ -actinin dimer and do not take into account collective binding effects, and/or to the forces

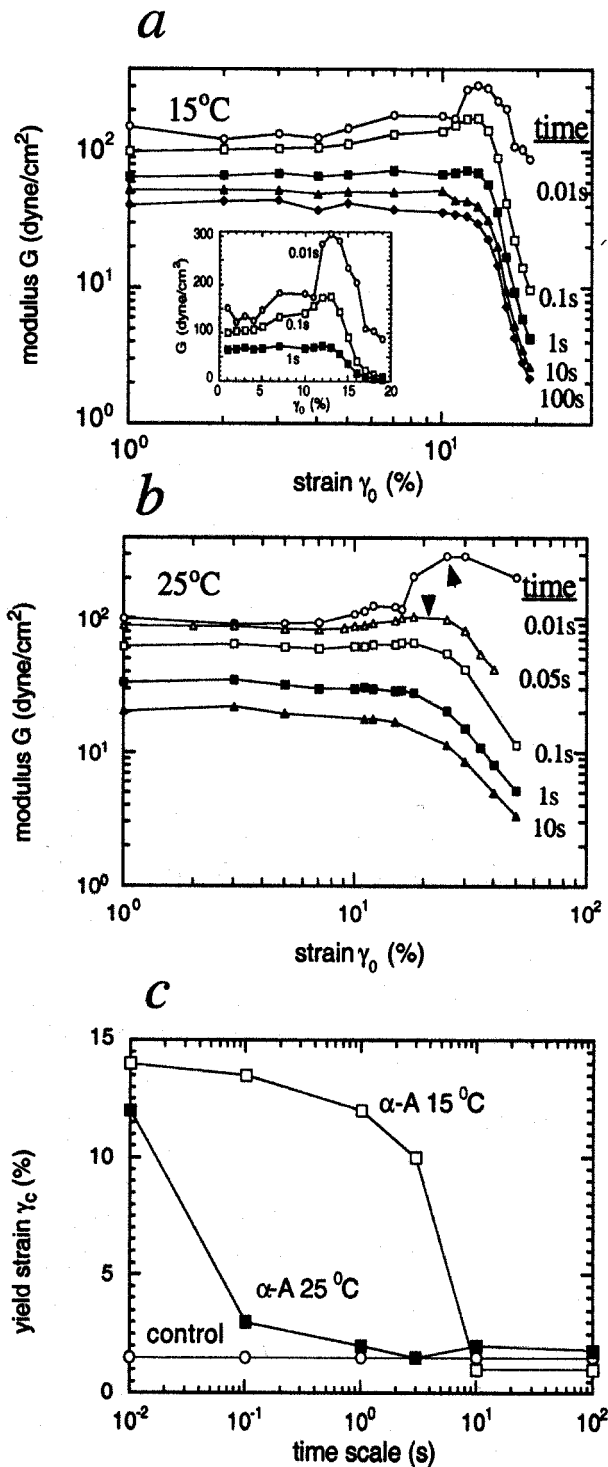


**FIG. 4. Strain-dependent modulus and yield strain of F-actin/ $\alpha$ -actinin networks.** The conditions for *a–c* were 24  $\mu$ M actin + 0.48  $\mu$ M  $\alpha$ -actinin in buffer F. Symbols in *a* and *b* correspond to probe time scales: 0.01 s ( $\circ$ ), 0.05 s ( $\Delta$ ), 0.1 s ( $\square$ ), 1 s ( $\blacksquare$ ), 10 s ( $\blacktriangle$ ), and 100 s ( $\blacklozenge$ ). *a*, shear modulus,  $G$ , versus strain amplitude  $\gamma_0$  at 15°C for time scales ranging from 0.01 to 100 s. *Inset*, associated linear plot. *b*,  $G$  versus  $\gamma_0$  at 25°C for time scales ranging from 0.01 to 10 s. *c*, yield strain,  $\gamma_c$ , as a function of time scale. Symbols are: F-actin + 0.48  $\mu$ M  $\alpha$ -actinin at 15°C ( $\square$ ), F-actin + 0.48  $\mu$ M  $\alpha$ -actinin at 25°C ( $\blacksquare$ ), and F-actin ( $\circ$ ). *a–c* were obtained from Fig. 3.

applied to the cross-linker, which are likely to increase the rates of dissociation (45). For time scales much longer than the lifetime of binding of  $\alpha$ -actinin to F-actin,  $1/k_{-}$ ,  $\alpha$ -actinin molecules at entanglements allow actin filaments to slide past one

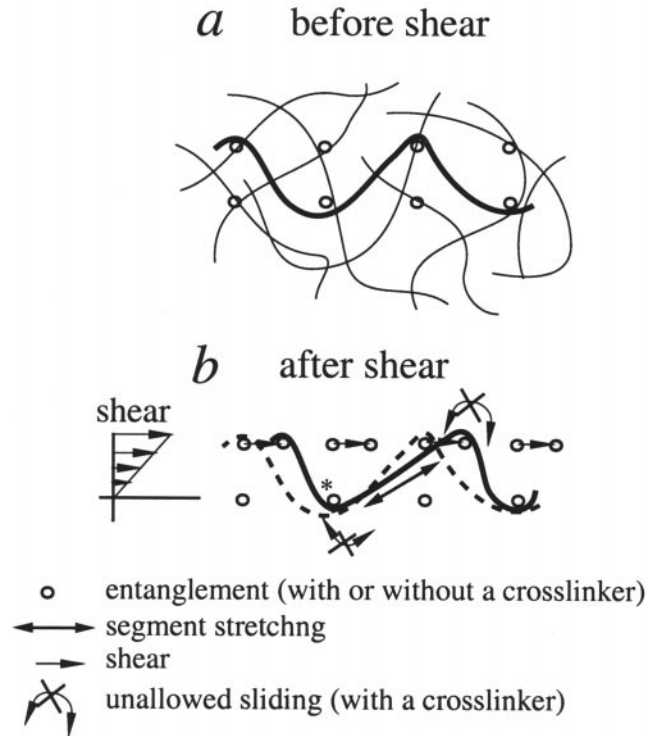


**FIG. 5. Model of strain hardening in F-actin gels.** *a*, a “test” actin filament (thick curve) is embedded in an entangled F-actin network (thin curves). Entanglements with surrounding filaments form a tube-like region inside which the test filament is initially confined.  $\alpha$ -Actinin molecules localize at those entanglement points. *b*, shape of the test filament after a step-shear deformation. The circles correspond to the entanglements in *a*; stars correspond to points of unfavorable bending of polymer segments, which induces strain hardening; the double-headed arrow indicates stretching of a section of filament, which becomes highly restricted in the presence of  $\alpha$ -actinin at low temperature and further enhances strain hardening. See text for more details.

another. This in turn allows stress relaxation, which is also supported by our results (Fig. 4). Our model of strain hardening also predicts that flexible polymers such as intermediate filaments in the presence of cross-linking proteins (e.g. plectin and keratin (28)) will exhibit enhanced strain hardening for rates of shear higher than the inverse of the dissociation constant of that cross-linking protein for the polymer, which remains to be tested (32).

**Implications for the Cell**—Using RGD peptide-coated beads and a magnetic twisting technique, Wang *et al.* (9) showed that applying shear stresses on cell integrin receptors resulted in an increase of cytoskeleton stiffness. However, Bausch *et al.* (10), who used FN-coated beads displaced by magnetic tweezers, observed no strain hardening; instead the cytoskeleton yielded, for deformation amplitudes of  $\gamma_c \approx 5\%$ , a yield strain similar to that observed here with reconstituted networks. A direct comparison between these two experiments is difficult, because the type of cell (NIH 3T3 murine fibroblasts *versus* bovine capillary endothelial cells) and the amplitude (small *versus* large) and type of deformations (twist *versus* shear) used were different. But our results suggest that the cytoskeleton could both strain-harden *and* strain-soften depending on the rate and amplitude of the applied strain. Our own preliminary observations with human foreskin fibroblasts and HeLa cells indicate that calibrated forces applied by FN-coated microneedles can indeed induce both hardening and softening of the cytoskeleton,<sup>2</sup> which helps reconcile these apparently contradictory results.

<sup>2</sup> Y. Tseng, A. Rahman, and D. Wirtz, unpublished data.

What is a possible molecular origin of strain hardening? RGD-coated beads (or, similarly, FN-coated beads) placed on the plasma membrane become readily anchored to the membrane via integrin cell receptors. Upon aggregation and ligand binding, integrins recruit cytoskeleton proteins (11), including F-actin and the actin-binding proteins vinculin, talin, tensin, and  $\alpha$ -actinin (12). Our results together with these observations therefore suggest a molecular model that might explain the origin of cytoskeleton strain hardening observed *in vivo* (9). Placing an FN-coated bead on the plasma membrane recruits F-actin and  $\alpha$ -actinin (as well other F-actin cross-linking proteins) (12), which subsequently cross-links F-actin. Twisting the bead induces unfavorable bending of actin filaments (see Fig. 5), which cannot slide past one another at cross-linking points due to  $\alpha$ -actinin (and/or other F-actin cross-linking proteins). This in turn causes strain hardening of the cytoskeleton. Note that *in vivo* measurements of cell rheology (9, 10, 46)<sup>3</sup> indicate that the system F-actin +  $\alpha$ -actinin is not sufficient to reconstitute the full mechanical response of the cell. Both the levels of elasticity at low strain amplitudes and the extent of strain hardening at high strains are higher in live cells. This indicates that other structural proteins such as bundling and cross-linking proteins may be required (47).

Severing and capping of F-actin, as well as *de novo* polymerization of actin, which are mediated by actin-binding proteins, are exploited by adherent cells to modify the local organization and associated physical properties of the actin cytoskeleton (48, 49). The expression of a large number of structural proteins seems to be triggered/enhanced by mechanical stresses; albeit, often at a slow pace after application of the stress (50–53). This would be unsuitable for a timely response to a shear stress suddenly applied to the cell. Our results, obtained with reconstituted F-actin networks, suggest that when stresses are small, the supplemental stiffness of the actin cytoskeleton provided by F-actin cross-linkers such as  $\alpha$ -actinin can be immediately used to stabilize the cytoskeleton and focal adhesions against further mechanical perturbations. When the shear stress is higher than a threshold value, the F-actin network softens, which may in turn help coordinate cytoskeleton reorganization required for cell motion and/or spreading (54). This may provide the cell with a passive mechanism (*i.e.* which requires neither increased levels of protein expression nor enzymatic reactions) to instantaneously sort out and exploit intracellular and extracellular deformations. The cofactors that regulate the lifetime of binding of  $\alpha$ -actinin to F-actin, which are yet to be identified, would play the role of temperature in our experiments. Our model also predicts that the mechanical response of the cytoskeleton will depend not only on the extent, but also on the rate of shear: If the cytoskeleton is sheared slowly (corresponding to time scales much longer than the lifetime of binding of the cross-linkers), because filaments can slide past one another, strain hardening should be small. *Vice versa*, if the cytoskeleton is sheared rapidly, strain hardening is enhanced because filaments do not have sufficient time to slide past one another. The extent of involvement of  $\alpha$ -actinin and other actin cross-linking proteins in cytoskeleton strain hardening and our model can be tested *in vivo* by 1) using mutant cells lacking  $\alpha$ -actinin or other actin cross-linking proteins (55) and 2) using instruments recently used to apply mechanical stresses and measure the viscoelastic properties of the cytoskeleton in living cells (9, 10, 46, 56–58).

*Acknowledgments*—We acknowledge insightful conversations with

T. D. Pollard, P. A. Coulombe, L. Ma, S. Yamada, and T. C. B. McLeish.

## REFERENCES

- Cramer, L. P., Mitchison, T. T., and Theriot, J. A. (1994) *Curr. Opin. Cell Biol.* **6**, 62–86
- Yamada, K. M., and Miyamoto, S. (1995) *Curr. Opin. Cell Biol.* **7**, 681–689
- Johnson, R. P., and Craig, S. W. (1996) *Curr. Opin. Cell Biol.* **8**, 74–85
- Huang, S., and Ingber, D. E. (1999) *Nature Cell Biol.* **1**, E131–E138
- Konstantopoulos, K., and McIntire, L. V. (1996) *J. Clin. Invest.* **98**, 2661–2665
- Lum, B., and Malik, A. B. (1994) *Am. J. Physiol.* **267**, L223–L241
- Pollard, T. D., and Cooper, J. A. (1986) *Ann. Rev. Biochem.* **55**, 987–1035
- Almo, S., Pollard, T. D., Quirk, S., Vinson, V., and Lattman, E. E. (1994) *Ann. Rev. Cell Biol.* **10**, 207–249
- Wang, N., Butler, J. P., and Ingber, D. E. (1993) *Science* **260**, 1124–1127
- Bausch, A. R., Möller, W., and Sackmann, E. (1999) *Biophys. J.* **76**, 573–579
- Grinnell, F., and Geiger, B. (1986) *Exp. Cell Res.* **162**, 449–461
- Miyamoto, S., Akiyama, S. K., and Yamada, K. M. (1995) *Science* **267**, 883–885
- Ingber, D. E. (1997) *Ann. Rev. Physiol.* **59**, 575–599
- Palmer, A., Xu, J., Kuo, S. C., and Wirtz, D. (1999) *Biophys. J.* **76**, 1063–1071
- Janmey, P. A., Hvidt, S., Lamb, J., and Stossel, T. P. (1990) *Nature* **345**, 89–92
- Leinweber, B., Tang, J. X., Stafford, W. F., and Chalovich, J. M. (1999) *Biophys. J.* **77**, 3208–3217
- Janmey, P. A., Hvidt, S., Kas, J., Lerche, D., Maggs, A., Sackmann, E., Schliwa, M., and Stossel, T. P. (1994) *J. Biol. Chem.* **269**, 32503–32513
- Tang, J. X., Janmey, P. A., Stossel, T. P., and Ito, T. (1999) *Biophys. J.* **76**, 2208–2215
- Critchley, D. R. (1993) in *Guidebook to the Cytoskeletal and Motor Proteins* (Kreis, T., and Vale, R., eds) pp. 22–23, Oxford University Press, Oxford
- Xu, J., Wirtz, D., and Pollard, T. D. (1998) *J. Biol. Chem.* **273**, 9570–9576
- Sato, M., Schwarz, W. H., and Pollard, T. D. (1987) *Nature* **325**, 828–830
- Wachsstock, D., Schwarz, W. H., and Pollard, T. D. (1994) *Biophys. J.* **66**, 801–809
- Spudich, J. A., and Watt, S. (1971) *J. Biol. Chem.* **246**, 4866–4871
- MacLean-Fletcher, S. D., and Pollard, T. D. (1980) *J. Cell Biol.* **85**, 414–428
- Isambert, H., Venier, P., Maggs, A. C., Fattoum, A., Kassab, R., Pantaloni, D., and Carlier, M.-F. (1995) *J. Biol. Chem.* **270**, 11437–11444
- Craig, S. W., Lancashire, C. L., and Cooper, J. A. (1982) *Methods Enzymol.* **85**, 316–321
- Xu, J., Schwarz, W. H., Kas, J., Janmey, P. J., and Pollard, T. D. (1998) *Biophys. J.* **74**, 2731–2740
- Ma, L., Xu, J., Coulombe, P. A., and Wirtz, D. (1999) *J. Biol. Chem.* **274**, 19145–19151
- Wachsstock, D., Schwarz, W. H., and Pollard, T. D. (1993) *Biophys. J.* **65**, 205–214
- Grazi, E., Cuneo, P., Magri, E., Schwienbacher, C., and Trombetta, G. (1993) *Biochemistry* **32**, 8896–8901
- Ferry, J. D. (1980) *Viscoelastic Properties of Polymers*, John Wiley and Sons, New York
- Coulombe, P. A., Bousquet, O., Ma, L., Yamada, S., and Wirtz, D. (2000) *Trends Cell Biol.* **10**, 420–428
- Doi, M., and Edwards, S. F. (1989) *The Theory of Polymer Dynamics*, Clarendon Press, Oxford
- Morse, D. C. (1998) *Phys. Rev. E* **58**, R1237–R1240
- Palmer, A., Xu, J., and Wirtz, D. (1998) *Rheologica Acta* **37**, 97–108
- Xu, J., Palmer, A., and Wirtz, D. (1998) *Macromolecules* **31**, 6486–6492
- Isambert, H., and Maggs, A. C. (1996) *Macromolecules* **29**, 1036–1040
- Gittes, F., and MacKintosh, F. C. (1998) *Phys. Rev. E* **58**, R1241–R1244
- Schnurr, B., Gittes, F., MacKintosh, F. C., and Schmidt, C. F. (1997) *Macromolecules* **30**, 7781–7792
- Hinner, B., Tempel, M., Sackmann, E., Kroy, K., and Frey, E. (1998) *Phys. Rev. Lett.* **81**, 2614–2617
- Letierrier, J. F., Kas, J., Hartwig, J., Vegners, R., and Janmey, P. A. (1996) *J. Biol. Chem.* **271**, 15687–15694
- Gittes, F., Mickey, B., Nettleton, J., and Howard, J. (1993) *J. Cell Biol.* **120**, 923–934
- Mason, T. G., Dhople, A., and Wirtz, D. (1998) *Macromolecules* **31**, 3600–3603
- Kuhlman, P. A., Ellis, J., Critchley, D. R., and Bagshaw, C. R. (1994) *FEBS Lett.* **339**, 297–301
- Miyata, H., Yasuda, R., and Kinosita, K., Jr. (1996) *Biochim. Biophys. Acta* **1290**, 83–88
- Yamada, S., Wirtz, D., and Kuo, S. C. (2000) *Biophys. J.* **78**, 1736–1747
- Apar, J., Tseng, Y., Federov, E., Herwig, M. B., Almo, S. C., and Wirtz, D. (2000) *Biophys. J.* **79**, 1095–1106
- Condeelis, J. (1992) *Cell Motil. Cytoskel.* **22**, 1–6
- Ayscough, K. R. (1998) *Curr. Opin. Cell Biol.* **10**, 102–111
- Girard, P. R., and Nerem, R. M. (1995) *J. Cell. Physiol.* **163**, 179–193
- Thoumine, O., Ziegler, T., Girard, P. R., and Nerem, R. M. (1995) *Exp. Cell Res.* **219**, 427–441
- Kano, Y., Katoh, K., Masuda, M., and Fujiwara, K. (1996) *Circ. Res.* **79**, 1000–1006
- Shyy, J. Y. J., and Chien, S. (1997) *Curr. Opin. Cell Biol.* **9**, 707–713
- Lauffenburger, D. A., and Horwitz, A. F. (1996) *Cell* **84**, 359–369
- Rivero, F., Koppel, B., Peracino, B., Bozzaro, S., Siegfert, F., Weijer, C. J., Schleicher, M., Albrecht, R., and Nogel, A. A. (1996) *J. Cell Sci.* **109**, 2679–2691
- Choquet, D., Felsenfeld, D. P., and Sheetz, M. P. (1997) *Cell* **88**, 39–48
- Thoumine, O., and Ott, A. (1997) *J. Cell Sci.* **110**, 2109–2116
- Heidemann, S. R., Kaech, S., Buxbaum, R. E., and Matus, A. (1999) *J. Cell Biol.* **145**, 109–122

<sup>3</sup> Y. Tseng, and D. Wirtz, unpublished results.